Anomalous in-plane magnetoresistance in a $EuFe_2As_2$ single crystal: Evidence of strong spin-charge-lattice coupling

Y. Xiao,[1,*] Y. Su,[2] S. Nandi,[1] S. Price,[1] B. Schmitz,[1] C. M. N. Kumar,[1] R. Mittal,[3] T. Chatterji,[4] N. Kumar,[5] S. K. Dhar,[5] A. Thamizhavel,[5] and Th. Brückel[1,2]

[1]*Jülich Centre for Neutron Science JCNS and Peter Grünberg Institute PGI, JARA-FIT, Forschungszentrum Jülich GmbH, 52425 Jülich, Germany*

[2]*Jülich Centre for Neutron Science, Forschungszentrum Jülich GmbH, Outstation at FRM II, Lichtenbergstraße 1, 85747 Garching, Germany*

[3]*Solid State Physics Division, Bhabha Atomic Research Centre, Trombay, Mumbai 400 085, India*

[4]*Institut Laue-Langevin, B.P. 156, 38042 Grenoble Cedex, France*

[5]*Department of Condensed Matter Physics and Material Sciences, Tata Institute of Fundamental Research, Homi Bhabha Road, Colaba, Mumbai 400 005, India*

(Received 28 October 2011; published 5 March 2012)

In-plane magnetotransport properties of a $EuFe_2As_2$ single crystal are investigated by angular-dependent magnetoresistance (MR) measurements. Strong anisotropy in magnetotransport properties is observed below the magnetic ordering temperature and it exhibits intimate correlations with the ordering states of both Eu^{2+} and Fe^{2+} spins as well as the twinned structure in $EuFe_2As_2$ crystal. Such correlations lead to giant MR effect around the magnetic phase boundary, e.g., negative MR of ∼26% is observed at 5 K and 1 T upon the reorientation of Eu^{2+} spins from antiferromagnetic to ferromagnetic configuration. Compared with Eu^{2+} moments, Fe^{2+} moments with antiferromagnetic arrangement generated relatively weak effect on MR due to its small ordered moment. All obtained MR results can be well understood based on the scenario of superzone boundary effect and the electron scattering by fluctuation of spins and twinning boundaries. It also suggests that the magnetic order state plays an important role for the determination of transport properties through the strong coupling between itinerant electrons and ordered spins.

DOI: 10.1103/PhysRevB.85.094504 PACS number(s): 74.70.Xa, 74.62.−c, 75.47.−m, 75.25.Dk

I. INTRODUCTION

The discovery of iron pnictide superconductors with transition temperature up to 56 K has attracted extensive interest on their physical properties and thereby the physical mechanism of high-temperature superconductors.[1,2] The undoped iron pnictides are not superconducting under ambient pressure and show an antiferromagnetic (AFM) spin-density wave (SDW) order.[3,4] Upon carrier doping or application of static pressure, the magnetic order is suppressed and superconductivity emerges concomitantly.[5,6] It is believed that the suppression of the AFM SDW order in the undoped compounds is the key to reach high-temperature superconductivity. Among the iron arsenide AFe_2As_2 (with A = Ba, Ca, or Sr etc.) family, $EuFe_2As_2$ stands out as a special system since the a site is occupied by Eu^{2+}, which is an S-state rare-earth ion possessing $4f^7$ electrons with the total electron spin $S = 7/2$.[7,8] Works on $EuFe_2As_2$ single crystals revealed that the Fe and Eu spins form long-range AFM order below 190 and 19 K, respectively.[9] Furthermore, the application of an external magnetic field will induce a magnetic phase transition in $EuFe_2As_2$ with the Eu moments changing from AFM to FM arrangement,[10] while the AFM SDW order of Fe is found to be robust and it persists in the investigated field range up to 3 T.[11] The superconductivity can be achieved by applying high pressure or doping on any site in $EuFe_2As_2$.[12–21]

Given the fact that a large in-plane electronic anisotropy exists in the AFM phase,[22–24] it is significant to understand the relationship between magnetism and electrical property of iron pnictide system. The magnetoresistance (MR) is a useful probe that can provide insight into the peculiar coupling between the charge carriers and the spin system.[25–27] In this paper, we show angular-dependent in-plane magnetoresistance (AMR) measurements for a $EuFe_2As_2$ single crystal. In-plane electronic anisotropy and the crossover of AMR are clearly observed due to the strong couplings between the itinerant electrons, ordered spins, and twinned lattices.

II. EXPERIMENT

Resistivity (ρ) measurements were performed by using the four-probe method on a high-quality $EuFe_2As_2$ single crystal. The current (I) direction was along orthorhombic a/b axis due to existence of twinned structure. Angular dependence of magnetoresistance measurements were carried out at constant temperature by rotating the sample around the c axis in a magnetic field (H) confined in the ab plane [see Fig. 2(a)]. The angle θ between magnetic field and a/b axis varies from 0 to 360°. The magnetoresistance is defined as $MR = [\rho(T,\theta,H) - \rho(T,\theta,H = 0)]/\rho(T,\theta,H = 0)$.

III. RESULTS AND DISCUSSION

Temperature dependence of zero-field resistivity for $EuFe_2As_2$ is shown in Fig. 1. Two anomalies, associated with structural/SDW transition (T_S/T_N^{Fe}) and AFM transition (T_N^{Eu}) of Eu^{2+} are observed at 190 and 19 K, respectively. In order to demonstrate the effect of magnetic field on charge transport in $EuFe_2As_2$ crystal, the $\rho(T)$ data measured at 9 T with applied field parallel and perpendicular to current direction are plotted together with zero-field resistivity data in Fig. 1. It can be seen that the structural/SDW transitions persist at 190 K and almost no magnetoresistance effect is observed above T_S. While in low-temperature region, the

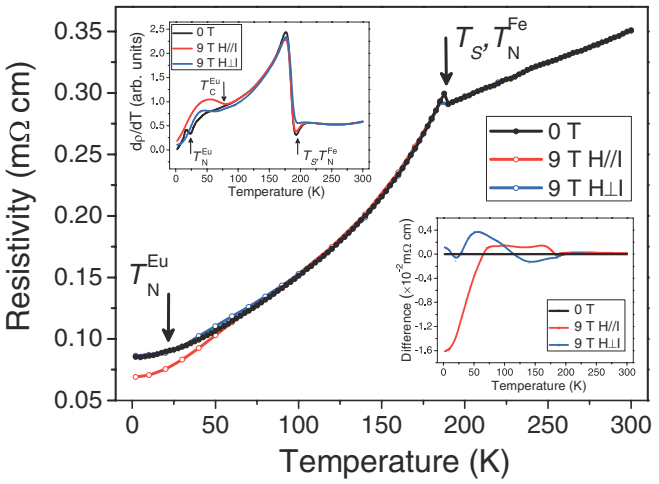

FIG. 1. (Color online) Temperature dependence of in-plane resistivity for $EuFe_2As_2$ single crystal at 0 T and 9 T with magnetic field parallel and perpendicular to current directions. The current direction is parallel to the orthorhombic a/b axes. Top-left inset shows the deviation of the resistivity as a function of temperature. Arrows indicate the AFM ordering temperature of Eu (T_N^{Eu}) and Fe (T_N^{Fe}) as well as the FM ordering temperature of T_C^{Eu}. The ordering temperature is defined as the local minimal from the deviation of the resistivity. The difference between the resistivity measured at 9 T and 0 T is plotted in bottom-right inset.

resistivities measured under 9 T field deviate from zero-field resistivity, which suggests the existence of a considerable magnetoresistance effect. In addition, the ordering temperature of Eu^{2+} moments increases to high temperature (~75 K) as revealed in the temperature derivatives of the resistivity data (top-left inset of Fig. 1). It is also noticed that the resistivity differences $[\rho_{\mathrm{Diff}} = \rho(H = 9\ \mathrm{T}) - \rho(H = 0\ \mathrm{T})]$ induced by applied magnetic field are quite different for $H||I$ and $H\perp I$, as shown in the bottom-right inset of Fig. 1. At 2 K, negative in-plane MR is observed with the field parallel to current, while slightly positive in-plane MR exists at 2 K with the field perpendicular to the current. This suggests that the scattering manner of charges is variant with respect to the angle between field and current.

In order to study the effect of applied field on the anisotropy of in-plane MR systematically, we investigated the angular dependence of MR at different temperatures and different fields. A simple sketch of experimental geometry for AMR measurement is given in Fig. 2(a). Interesting features are clearly observed in AMR(θ) measurement of $EuFe_2As_2$ at 2 K and different applied fields, as shown in Fig. 2(b). First, the AMR exhibits a twofold symmetry even under a low-magnetic field of 0.2 T. The oscillation of MR with different angles between H and I can be attributed to the anisotropic scattering of charge carriers by magnetic moments. Second, the angular dependence of magnetoresistance becomes complicated around 0.5 T. The polar plot of AMR at 0.5 T exhibits a d-wavelike behavior as shown in Fig. 2(c). The redistribution of the twinned structure in $EuFe_2As_2$ can account for this d-wavelike behavior and it will be discussed in the following text. Third, a crossover of AMR is observed with further increase in magnetic field above the critical field of ~0.7 T. The relative strength of MR between $H||I$ and $H\perp I$ reverses from this critical field. Moreover, the two-fold symmetry still persists at a high magnetic field region. Indeed, the field-induced spin-flop transition of Eu^{2+} spins from AFM to FM at 2 K and ~0.7 T has been observed by our neutron diffraction study.[11] Therefore, the dramatic change of AMR magnitude around 0.7 T can be considered as the response of the transport property of $EuFe_2As_2$ to different spin configurations. AMR results clearly indicate that the charge carriers interact intimately with spins and the interaction between them plays an important role for the AMR of the $EuFe_2As_2$ compound.

Besides of spin-charge coupling effect, the influence of twinned structure on AMR results can also not be neglected since twinning boundaries will present as planar defects and conduction electrons can be scattered by these defects. As shown in Ref. 11, the twinned structure will inevitably emerge in the orthorhombic phase of $EuFe_2As_2$ and the twinned crystal can be detwinned by applying external field due to spin-lattice coupling. At 2 K, the detwinning process starts at a lower critical field of ~0.4 T and accomplishes at a higher critical field of ~0.7 T. A schematic view of the twinned structure in orthorhombic phase without field is shown in Fig. 3(a). Four different domain patterns are coexisting and the overall structure is still an average tetragonal lattice as revealed by its diffraction patterns.[9,28] Below the lower critical field of ~0.4 T, there is almost no change in the twinned structure compared with its zero-field pattern. As an example, AMR at 0.2 T and 2 K is plotted in polar coordinates in Fig. 2(c). The p-wavelike behavior of AMR can be attributed to the anisotropic scattering of charge carriers by magnetic moments, which also indicates that the twinning boundary scattering has negligible effect on magnetoresistance at the low magnetic field region. Once the field increases above the lower critical field, the twinned crystal will be partially detwinned, i.e., some $(0k0)$ twins overcome domain-wall energy and are realigned to *(h00)* twins, as illustrated in Fig. 3(b). The detwinning process will reduce the overall lattice symmetry and the d-wavelike behavior of AMR at 0.5 T reflects the change of twin patterns [Fig. 2(c)]. With further increase in field, the crystal will be totally detwinned by the external magnetic field and the twin boundary disappears consequently [see Fig. 3(c)]. As a result, a 90°-rotated p-wavelike behavior is observed for AMR at 3 T [see Fig. 2(c)]. In Fig. 2(d), θ angle is swept forward and backward during the AMR measurement at 0.5 and 3 T. It is clear that both magnetic moment scattering and twinning boundary scattering processes will lead to the oscillations of MR with different angles between applied field and current. Interestingly, it is noticed that these two scattering processes exhibit different hysteresis behaviors. As evidenced by AMR data obtained at 0.5 T, considerable hysteresis in AMR is observed in θ range between −60° and 60°, which indicated that the moment scattering process is dominated in this region. While in θ range between 60° and 120°, almost no detectable hysteresis is shown, which indicated that the twin boundary scattering process is dominated.

Figure 4(a) shows in-plane MR at different temperatures with $H||I$. It is obvious that the MR exhibits different behaviors in different temperature ranges. At 5 K, MR increases slightly and reach a maximum of ~3% at 0.3 T, then it exhibits a steplike decrease with further increase of applied field [see Fig. 4(b)]. The MR value drops down

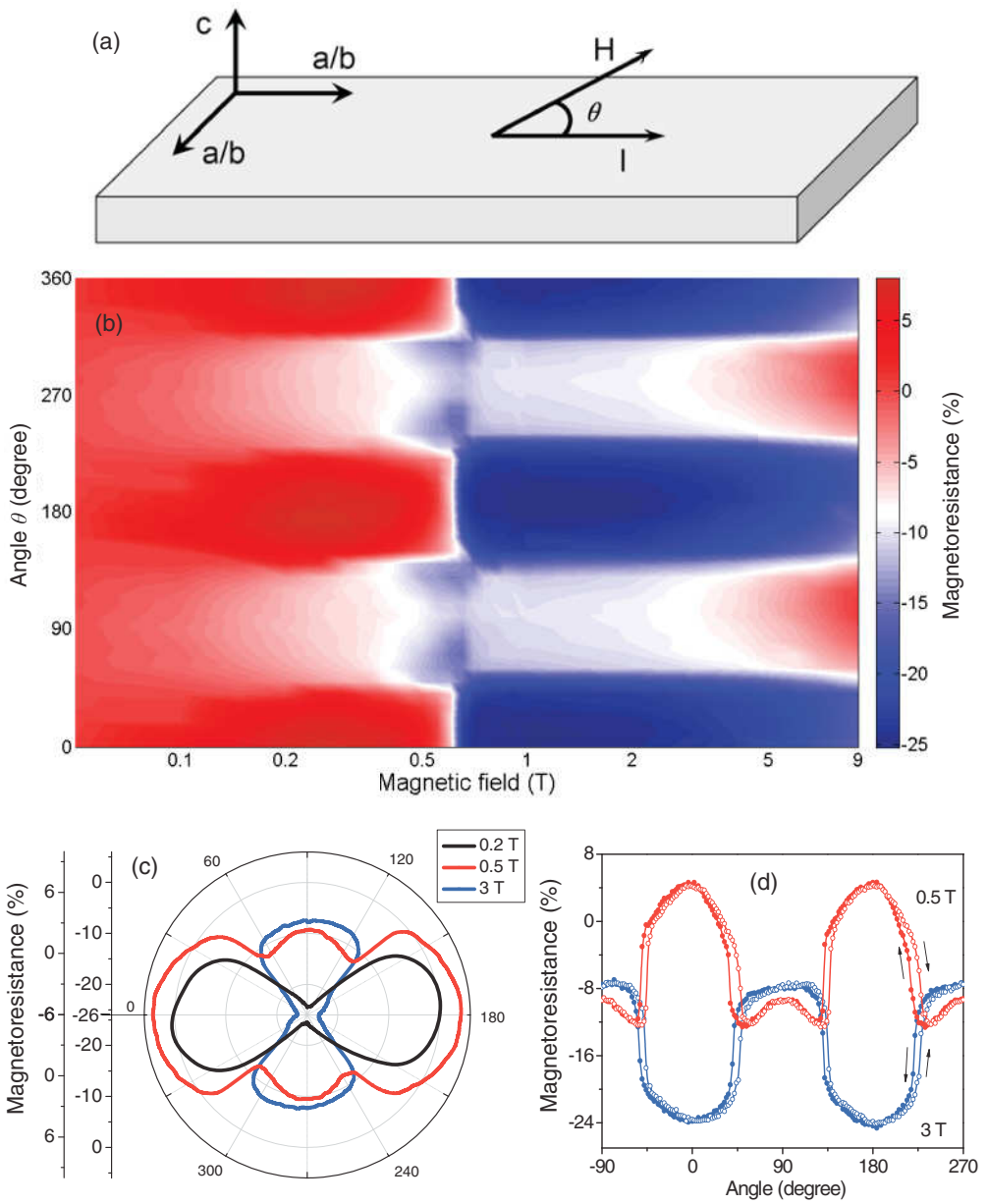

FIG. 2. (Color online) (a) Schematic view of the geometry of AMR experiment. (b) Angular dependence of magnetoresistance for $EuFe_2As_2$ at 2 K. The logarithmic scale is adopted for magnetic field axis in order to illustrate the features clearly in the lower magnetic field range. (c) Angular dependencies of MR at 0.2 T, 0.5 and 3 T are plotted in polar coordinates. The radial coordinate for AMR data at 0.2 T is given as the vertical axis in the left side, while the vertical axis in the right side is for AMR data collected at 0.5 and 3 T. (d) The angular dependencies of MR at 0.5 and 3 T are plotted in linear coordinates with θ angle swept forward and backward.

to $\sim -26\%$ at the critical field of ~ 0.7 T. Note that both slight increase at low field and sudden decrease around the threshold field are only observed for MR measurements below $T_N^{Eu} = 19$ K, whereas the low-field range is featureless when the temperature is greater than T_N^{Eu}, as shown in the enlarged view of the low-field range in Fig. 4(b). Apparently, both features are of spin origin and can be considered as the response of charge transport upon the change of ordering of Eu^{2+} spin moments. Yamada *et al.*[29] have investigated the resistivity of antiferromagnetic metals within the molecular field approximation. The resistivity due to the electron-spin scattering in a localized spin system can be expressed as $\rho(T,H) = \rho_{Longi}(T,H) + \rho_{Trans}(T,H)$, where ρ_{Longi} and ρ_{Trans} are the resistivities due to longitudinal and transverse spin fluctuations [see Eqs. (3.9) and (3.10) in Ref. 29], respectively. According to this theory, a positive MR will exist in the AFM state when the external magnetic field is applied parallel to the sublattice magnetization in the AF state. Therefore the initial increase of MR in curves [see Fig. 3(b)] with temperature lower than T_N^{Eu} is mainly attributed to the scattering of conduction electrons by the fluctuation of localized spins. The sudden decrease of MR around the critical field is associated with the spin reorientation transition of Eu^{2+} moment from AFM to FM configuration as aforementioned. It can be understood based

on the scenario of the superzone boundary effect.[30] Once the antiferromagnetic state is established, the magnetic superzone is generated and creates the energy gap. Consequently, the free-electron Fermi surface is deformed and the charge carrier density is reduced. Whereas in the ferromagnetic state, the superzone effect does not exist. As a result, the electrical resistivity drops sharply accompanied by the transition from antiferromagnetic to ferromagnetic state. In fact, a similar feature of decrease in MR is also observed in some other rare-earth transition metal compounds[31,32] due to the magnetic phase transition from antiferromagnetic to ferromagnetic state.

Above the critical field $H_{\rm crit}$, Eu moments align ferromagnetically. It is known that in ferromagnetic system the increase of effective field acting on the localized spins will suppress the spin fluctuations, which will lead to the decrease of magnetoresistance. However, the MR in FM state keep increasing with increasing applied field in our $EuFe_2As_2$ case although it still possesses a negative value. Therefore the cyclotron motion of charge carries, which will produce enhancement in resistivity in the presence of applied field, has to be taken into account.[33] The carrier scattering time (τ) and cyclotron frequency (ω) are two crucial factors in determination of the contribution of cyclotron motion to the change of MR. The carrier scattering time becomes larger at low temperature and the cyclotron frequency is also increased under the application of high magnetic field. Therefore, the contribution arising from cyclotron motion of charger carriers dominate the MR at low temperature and high magnetic fields. As a result, the MR increases linearly above the critical field.

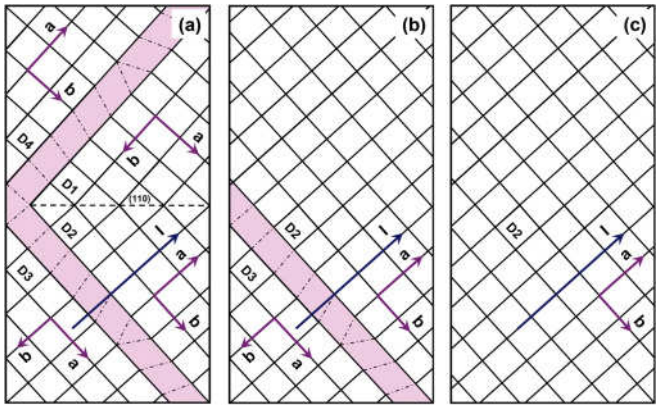

FIG. 3. (Color online) Schematic presentations of the evolution of twinned structure in orthorhombic *a*-*b* plane. Twinned structure emerges in orthorhombic phase accompanied with the formation of twinning boundaries (a). With increasing field, $EuFe_2As_2$ crystal is partially detwinned (b) and reaches single domain state (c) under high magnetic field. The vectors *a* and *b* denote *a* and *b* axes in orthorhombic structure. The direction of current *I* is also indicated by arrows.

By fitting the linear part of MR curve in the high field range, the slope of MR in FM phase is obtained and plotted in Fig. 4(c) as a function of temperature. The gradual decrease of slope indicated that the contribution to MR due to cyclotron motion is largely diminished with increasing temperature.

In Fig. 4(a), it can also be seen that MR at 9 T increases continuously with increasing temperature from $\sim -21\%$ (at

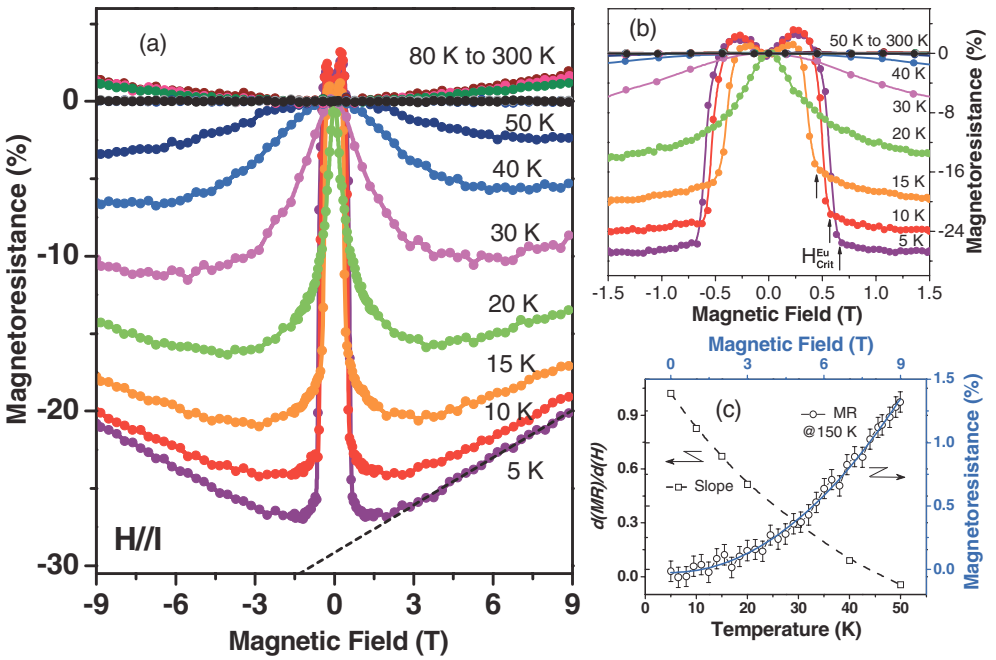

FIG. 4. (Color online) (a) The magnetoresistance of $EuFe_2As_2$ for magnetic field parallel to the current direction and orthorhombic *a*/*b* axis. A linear behavior is observed for the high field part below the Eu ordering temperature. Representative fitting of the linear behavior is shown for $T = 5$ K as the dashed line. (b) Enlarged views of (a) around low field. Kinks are observed for curves measured below $T_N^{\rm Eu}$ (19 K). The magnetic fields corresponding to the kinks are defined as critical fields $H_{\rm crit}^{\rm Eu}$, which reflects the change of Eu spins from AFM to FM arrangement. (c) Cubics and dashed line: temperature dependence of the slope of the linear part of MR data in (a). Circles and full line: Enlarged view of MR data at 150 K.

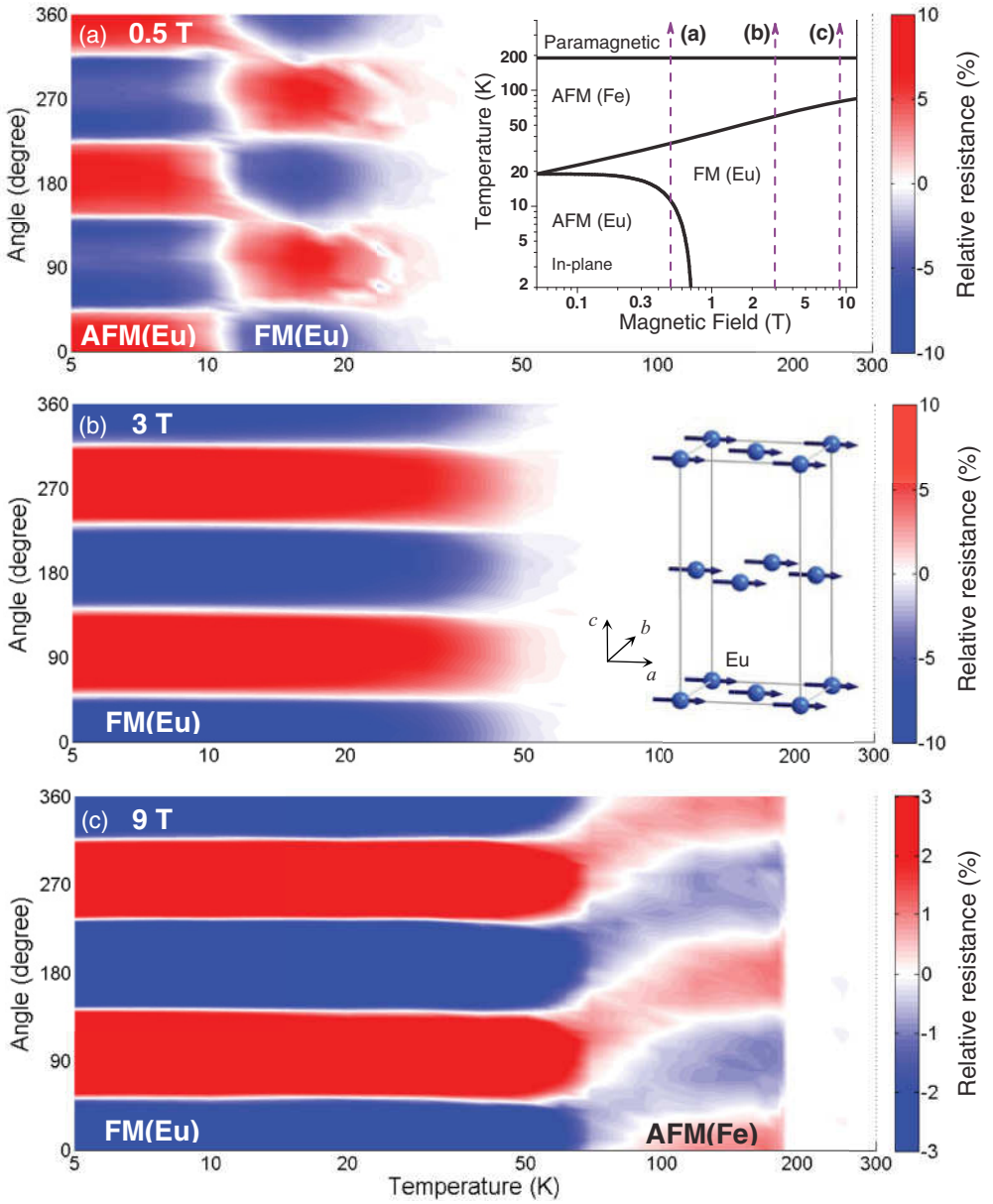

FIG. 5. (Color online) Temperature dependence of AMR at (a) 0.5, (b) 3, and (c) 9 T. In order to illustrate the evolution of AMR clearly, here we defined relative resistance (RR) as $RR = [R(T,\theta,H) - \overline{R(T,\theta,H)}]/\overline{R(T,\theta,H)}$, where $\overline{R(T,\theta,H)}$ represents the average resistance over θ from 0 to 360° at finite temperature and magnetic field. The logarithmic scale is adopted for the temperature axis of all plots to address the low temperature features. Inset of (a) shows the in-plane magnetic phase diagram for $EuFe_2As_2$. Dotted lines mark the field used for AMR measurement of (a), (b), and (c). Inset of (b) shows the schematic view of the field-induced ferromagnetic spin structure of Eu^{2+} moments.

5 K) to ∼−3% (at 50 K), which is in consistent with the fact that the magnitude of Eu FM ordering moment keeps decreasing with increasing temperature. Positive MR is observed once temperature is higher than the Eu ordering temperature ($T_C^{Eu} \sim 75$ K) at 9 T. As an example, field dependencies of MR at 150 K is plotted in Fig. 4(c). The small positive value of ∼1.35% is obtained for MR at 9 T. Moreover, MR follows a B^2 dependent behavior [full line in Fig. 4(c)], which is similar to the MR behavior observed in $Ba(Fe_{1-x}Co_x)_2As_2$.[34] The MR effect is not detectable once the temperature exceeds the Fe ordering temperature ($T_N^{Fe} = 190$ K). All these results suggests that the positive MR value in the temperature range ($\sim 75\text{ K} \leqslant T \leqslant \sim 190$ K) can mainly be attributed to the survival of antiferromagnetic order of Fe.

We have already shown that the angular dependence of magnetoresistance can be used as an effective probe for different ordering configurations. However, the AMR in all magnetic phases and the response of AMR to AFM SDW of Fe moments are still not clear. Thus the temperature dependence of AMR under three representative applied fields (0.5, 3, and 9 T) are shown in Fig. 5. Under 0.5 T, the reverse of AMR clearly marks the transition of Eu spin configuration from AFM to FM at ∼11 K. The AMR effect disappears at $T_C^{Eu} \sim 33$ K, where Eu^{2+} spin enter the paramagnetic disordered state. According to Yamada's theory,[29] the MR with $H||M$ is larger than that

with $H \perp M$ in the AFM state. Here, the M denotes the moment direction of magnetic system. In the FM state, the fluctuation of the spins will be suppressed with $H||M$, while it may increase when $H \perp M$. The suppression of fluctuation will result in smaller MR for $H||M$ in FM state. In present $EuFe_2As_2$ case, Eu spins are aligned along a axis in both AFM and FM phases. Therefore the reversion of MR at ~11 K [see Fig. 5(a)] can be well understood as the different responses of MR upon the change of different spin configurations. It should be noted that although the AFM order of Fe moment still survives below T_N^{Fe} (~190 K), the MR effect due to the AFM order of Fe moment at 0.5 T is too low to be detected. At 3 T, the FM arrangement of Eu moments is induced by the applied magnetic field. The T_C^{Eu} of Eu magnetic sublattice is detected to be ~60 K, as shown in Fig. 5(b). At 9 T, the ordering temperature of Eu spins is enhanced to $T_C^{Eu} \sim 75$ K, while the AMR that originated from Fe AFM SDW order dominates at higher temperature range $T_C^{Eu} < T < T_N^{Fe}$. Within the framework of spin fluctuations theory,[29] MR can be expressed as function of magnetic field and magnitude of magnetic moment. Given the fact that the magnitude of Fe moment is much smaller than that of Eu moment, the MR effect caused by interactions between electrons and Fe spins will be less than that of Eu counterpart. It is also noticed that the crossover of AMR evolutes gradually, which may be caused by the remaining order of Eu spins induced by the external magnetic field. Based on AMR results, we can easily determine the phase boundary and construct the in-plane phase diagram of $EuFe_2As_2$ as shown in the inset of Fig. 5(a).

IV. CONCLUSION

In summary, we have systematically studied the in-plane magnetotransport properties of a $EuFe_2As_2$ single crystal. Large (>25%) negative MR is observed at low temperature (<5 K) and small magnetic field (<2 T) when the magnetic field is parallel to the current direction and orthorhombic a/b axis. The origin of the anomalous MR effect can be well explained based on spin fluctuations and superzone boundary theories. AMR(θ) with twofold symmetry is observed for all magnetic ordering states, including the AFM and FM states of Eu as well as the AFM state of Fe. The reversion of AMR takes place upon the magnetic phase transition, which provides a direct evidence of the coupling between itinerant electrons and ordered spins. Besides, the effect of twinned structure on AMR results is also observed, which reveals the existence of charge-lattice coupling.

*y.xiao@fz-juelich.de

[1] Y. Kamihara, T. Watanabe, M. Hirano, and H. Hosono, J. Am. Chem. Soc. **130**, 3296 (2008).

[2] David C. Johnston, Adv. Phys. **59**, 803 (2010), and references therein.

[3] C. de la Cruz, Q. Huang, J. W. Lynn, J. Li, W. Ratcliff II, J. L. Zarestky, H. A. Mook, G. F. Chen, J. L. Luo, N. L. Wang, and P. C. Dai, Nature (London) **453**, 899 (2008).

[4] Y. Su, P. Link, A. Schneidewind, Th. Wolf, P. Adelmann, Y. Xiao, M. Meven, R. Mittal, M. Rotter, D. Johrendt, Th. Brueckel, and M. Loewenhaupt, Phys. Rev. B **79**, 064504 (2009).

[5] J. Zhao, Q. Huang, C. de la Cruz, S. Li, J. W. Lynn, Y. Chen, M. A. Green, G. F. Chen, G. Li, Z. Li, J. L. Luo, N. L. Wang, and P. Dai, Nat. Mater. **7**, 953 (2008).

[6] S. Nandi, M. G. Kim, A. Kreyssig, R. M. Fernandes, D. K. Pratt, A. Thaler, N. Ni, S. L. Bud'ko, P. C. Canfield, J. Schmalian, R. J. McQueeney, and A. I. Goldman, Phys. Rev. Lett. **104**, 057006 (2010).

[7] R. Marchand and W. Jeitschko, J. Solid State Chem. **24**, 351 (1978).

[8] H. Raffius, M. Moersen, B. D. Mosel, W. Mueller-Warmuth, W. Jeitschko, L. Terbuechte, and T. Vomhof, J. Phys. Chem. Solids **54**, 135 (1993).

[9] Y. Xiao, Y. Su, M. Meven, R. Mittal, C. M. N. Kumar, T. Chatterji, S. Price, J. Persson, N. Kumar, S. K. Dhar, A. Thamizhavel, and Th. Brueckel, Phys. Rev. B **80**, 174424 (2009).

[10] S. Jiang, Y. Luo, Z. Ren, Z. Zhu, C. Wang, X. Xu, Q. Tao, G. Cao, and Z. Xu, New J. Phys. **11**, 025007 (2009).

[11] Y. Xiao, Y. Su, W. Schmidt, K. Schmalzl, C. M. N. Kumar, S. Price, T. Chatterji, R. Mittal, L. J. Chang, S. Nandi, N. Kumar, S. K. Dhar, A. Thamizhavel, and Th. Brueckel, Phys. Rev. B **81**, 220406(R) (2010).

[12] N. Kurita, M. Kimata, K. Kodama, A. Harada, M. Tomita, H. S. Suzuki, T. Matsumoto, K. Murata, S. Uji, and Taichi Terashima, Phys. Rev. B **83**, 214513 (2011).

[13] K. Matsubayashi, K. Munakata, M. Isobe, N. Katayama, K. Ohgushi, Y. Ueda, Y. Uwatoko, N. Kawamura, M. Mizumaki, N. Ishimatsu, M. Hedo, and I. Umehara, Phys. Rev. B **84**, 024502 (2011).

[14] H. S. Jeevan, Z. Hossain, D. Kasinathan, H. Rosner, C. Geibel, and P. Gegenwart, Phys. Rev. B **78**, 092406 (2008).

[15] S. Jiang, H. Xing, G. Xuan, Z. Ren, C. Wang, Z. A. Xu, and G. Cao, Phys. Rev. B **80**, 184514 (2009).

[16] Z. Guguchia, J. Roos, A. Shengelaya, S. Katrych, Z. Bukowski, S. Weyeneth, F. Murányi, S. Strässle, A. Maisuradze, J. Karpinski, and H. Keller, Phys. Rev. B **83**, 144516 (2011).

[17] I. Nowik, I. Felner, Z. Ren, G. Cao, and Z. Xu, New J. Phys. **13**, 023033 (2011).

[18] Z. Ren, Q. Tao, S. Jiang, C. Feng, C. Wang, J. Dai, G. Cao, and Z. Xu, Phys. Rev. Lett. **102**, 137002 (2009).

[19] H. S. Jeevan, D. Kasinathan, H. Rosner, and P. Gegenwart, Phys. Rev. B **83**, 054511 (2011).

[20] D. Wu, G. Chanda, H. S. Jeevan, P. Gegenwart, and M. Dressel, Phys. Rev. B **83**, 100503(R) (2011).

[21] S. Zapf, D. Wu, L. Bogani, H. S. Jeevan, P. Gegenwart, and M. Dressel, Phys. Rev. B **84**, 140503(R) (2011).

[22] T.-M. Chuang, M. P. Allan, J. Lee, Y. Xie, Ni Ni, S. L. Budko, G. S. Boebinger, P. C. Canfield, and J. C. Davis, Science **327**, 181 (2010).

[23] J. Chu, J. Analytis, K. De Greve, P. McMahon, Z. Islam, Y. Yamamoto, and I. Fisher, Science **329**, 824 (2010).

[24] I. R. Fisher, L. Degiorgi, and Z. X. Shen, Rep. Prog. Phys. **74**, 124506 (2011).

[25] X. H. Chen, C. H. Wang, G. Y. Wang, X. G. Luo, J. L. Luo, G. T. Liu, and N. L. Wang, Phys. Rev. B **72**, 064517 (2005).

[26] S. Li, S. D. Wilson, D. Mandrus, B. Zhao, Y. Onose, Y. Tokura, and P. Dai, Phys. Rev. B **71**, 054505 (2005).
[27] T. Terashima, N. Kurita, A. Kikkawa, H. S. Suzuki, T. Matsumoto, K. Murata, and S. Uji, J. Phys. Soc. Jpn. **79**, 103706 (2010).
[28] M. A. Tanatar, A. Kreyssig, S. Nandi, N. Ni, S. L. Budko, P. C. Canfield, A. I. Goldman, and R. Prozorov, Phys. Rev. B **79**, 180508(R) (2009).
[29] H. Yamada and S. Takada, J. Phys. Soc. Jpn. **34**, 51 (1973).
[30] G. T. Meaden, Contemp. Phys. **12**, 313 (1971).
[31] A. K. Nigam, S. B. Roy, and P. Chaddah, Phys. Rev. B **60**, 3002 (1999).
[32] S. Radha, S. B. Roy, and A. K. Nigam, J. Appl. Phys. **87**, 6803 (2000).
[33] A. B. Pippard, *Magnetoresistance in Metals* (Cambridge University Press, Cambridge, England, 1989).
[34] J. H. Chu, J. G. Analytis, D. Press, K. DeGreve, T. D. Ladd, Y. Yamamoto, and I.R. Fisher, Phys. Rev. B **81**, 214502 (2010).